Nodal-knot semimetals

Ren Bi,[1] Zhongbo Yan,[1] Ling Lu,[2] and Zhong Wang[1,3,*]

[1]*Institute for Advanced Study, Tsinghua University, Beijing, 100084, China*
[2]*Institute of Physics, Chinese Academy of Sciences/Beijing National Laboratory for Condensed Matter Physics, Beijing 100190, China*
[3]*Collaborative Innovation Center of Quantum Matter, Beijing, 100871, China*

Topological nodal-line semimetals are characterized by one-dimensional lines of band crossing in the Brillouin zone. Unlike nodal points, nodal lines can be in topologically nontrivial configurations. In this paper, we study the simplest topologically nontrivial forms of nodal line, namely, a single nodal line taking the shape of a knot. They are dubbed "nodal-knot semimetals". A generic method of constructing various nodal knots is given, which generates the simplest trefoil nodal knot and other more complicated nodal knots in the Brillouin zone. Our work brings the knot theory to the subject of topological semimetals.

I. INTRODUCTION

Topological states have been under intense investigations in the last decade[1–5]. Topological semimetals[6] are characterized by topologically protected nodal points or nodal lines in the Brillouin zone, where the valance band and conduction band meet each other. The most extensively studied nodal-point semimetals are Weyl semimetals[7–21] and Dirac semimetals[22–30]. More recently, nodal-line semimetals have attracted considerable attention. Like the Dirac points, nodal lines[31–46] are protected by both the band topology and symmetries. There are quite a few material candidates of nodal lines; for instance, Cu_3NPd and Cu_3NZn[39, 40], Ca_3P_2[47, 48], Hg_3As_2[49], carbon networks[37], CaP_3[50], and alkali earth materials[51, 52]. Experimental studies of nodal lines are also in rapid progress[38, 53–58]. Nodal lines can be partially gapped, giving ways to Weyl semimetals. This phenomenon can occur due to the spin-orbit coupling or external driving[59–63].

Nodal points have little internal structure, for instance, the only topological characterization of a Weyl point is its chirality (±1). In contrast, nodal lines can have much richer topologically distinct possibilities. They can touch each other and form nodal chains[64, 65] stretching across the Brillouin zone [Fig.1(b)]. Another intriguing possibility is the nodal link[66–68], namely, two nodal lines topologically linked with each other [Fig.1(c)]. Links are also proposed in superconductors[69].

Nodal links are not the simplest topologically nontrivial shapes of nodal lines. The simplest shape contains only one nodal line entangled with itself, i.e., a knot. Such a nontrivial nodal line is dubbed a "nodal knot" in this paper, to distinguish it from the usual real-space knots. The simplest case is a trefoil nodal knot, shown in Fig.1(d). A crucial question is whether such a conception can exist in principle (i.e., can be explicitly constructed as models). The recently proposed method of constructing nodal links based on Hopf mappings cannot be applied to yield a nodal knot, because it necessarily produces multiple nodal lines. It is thus unclear whether a single-line nodal knot is realizable in materials. Here, we introduce a method based on functions of several complex
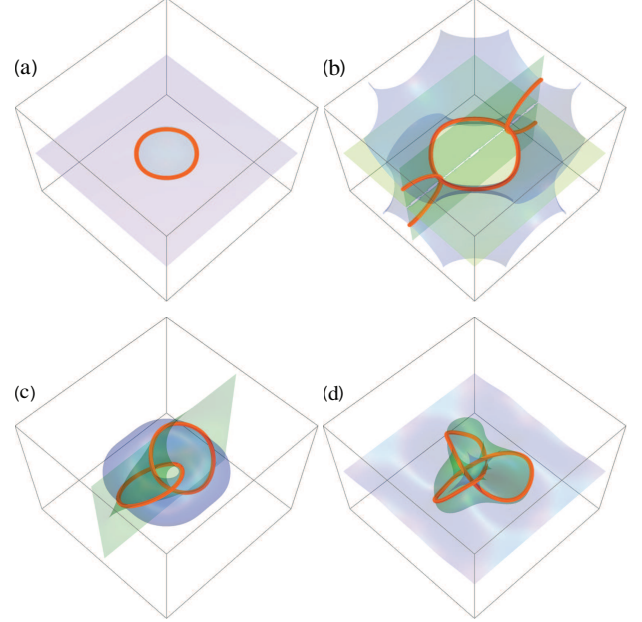

FIG. 1. Schematic illustration of four types of nodal line: (a) ordinary nodal line, (b) nodal chain, (c) nodal link, and (d) nodal knot. A nodal knot is a single nodal line entangled with itself. All nodal lines here are plotted as the intersections of two surfaces.

variables, which neatly gives various single-line nodal knots, including the trefoil knot as the simplest case. The topological transitions from the knotted configurations to trivial ones are also studied. Our work brings the extensively investigated knot theory[70] to the subject of topological semimetals.

II. CONTINUUM MODELS OF NODAL-KNOT SEMIMETALS

Nodal lines come from the crossing of two adjacent bands, thus we focus on two-band models below. Any two-band model can be written as

$$H(\mathbf{k}) = a_0(\mathbf{k})\mathbf{1} + a_1(\mathbf{k})\sigma_x + a_2(\mathbf{k})\sigma_y + a_3(\mathbf{k})\sigma_z, \quad (1)$$

where σ_i's are the Pauli matrices, and the trivial $a_0(\mathbf{k})$ term will be discarded below. Nodal lines are protected by the co-operation of band topology and certain symmetries[71–73].

In this work, we consider the combination[43, 74] of spatial-inversion symmetry $\mathcal{P}$ and time-reversal symmetry $\mathcal{T}$, which ensures that $H^*(\mathbf{k}) = H(\mathbf{k})$ up to a basis choice, thus we have $a_2(\mathbf{k}) = 0$. This $\mathcal{PT}$ symmetry is relevant to many material candidates of nodal lines (e.g., Cu_3PdN[39, 40], Cu_3TeO_6[75]). Given the symmetry, the Hamiltonian becomes

$$H(\mathbf{k}) = a_1(\mathbf{k})\sigma_x + a_3(\mathbf{k})\sigma_z, \tag{2}$$

whose energies are $E_\pm(\mathbf{k}) = \pm\sqrt{a_1^2(\mathbf{k}) + a_3^2(\mathbf{k})}$, and the nodal lines can be solved from $a_1(\mathbf{k}) = a_3(\mathbf{k}) = 0$. The most common choices of a_1 and a_3, say $a_1 = \cos k_x + \cos k_y + \cos k_z - m_0$, $a_3 = \sin k_z$, yield ordinary nodal lines resembling Fig.1(a). Taking advantage of the Hopf mappings[76–84], linked nodal lines can be constructed[67]. This method is sufficiently general to generate nodal links with any integer linking numbers (including the simplest Hopf link), however, it is unable to generate a nodal knot, which contains only one nodal line. This limitation is intrinsic in its construction[67].

In this paper, we introduce a general method to construct nodal knots based on functions of several complex variables. Before writing down the explicit models, we start from the geometrical preparations. Let us consider two complex variables z and w, with the constraint $|z|^2 + |w|^2 = 1$, which defines a 3-sphere. This is more transparent if we write $z = n_1 + in_2$ and $w = n_3 + in_4$, then $|z|^2 + |w|^2 = 1$ becomes $n_1^2 + n_2^2 + n_3^2 + n_4^2 = 1$, which is apparently a 3-sphere. For reasons to become clear shortly, let us consider the surface $|z|^p = |w|^q$ (where p, q are positive integers) in the 3-sphere. This surface is topologically a 2-torus. To see this fact, we notice that the two equations $|z|^2 + |w|^2 = 1$ and $|z|^p = |w|^q$ completely fix the values of $|z|$ and $|w|$, thus the surface can be parameterized by the phases θ_z and θ_w, which is defined in $z = |z|\exp(i\theta_z)$ and $w = |w|\exp(i\theta_w)$, respectively. Thus the surface is exactly a 2-torus, with θ_z and θ_w parameterizing the toroidal and poloidal direction, respectively.

Now we impose a constraint

$$f(z, w) \equiv z^p + w^q = 0. \tag{3}$$

The solutions (z, w) of this constraint must be on the torus $|z|^p = |w|^q$ discussed above, furthermore, the phases have to satisfy $p\theta_z - q\theta_w = \pi \pmod{2\pi}$. As a mathematic fact of torus geometry, when p and q are relatively prime, the equation defines only one line on the torus. Otherwise, we have multiple lines. For instance, when $(p, q) = (3, 2)$, we have a single line passing the point $(\theta_z, \theta_w) = (\pi/3, 0)$; when $(p, q) = (2, 4)$, we have two disconnected lines, one of which passes $(\theta_z, \theta_w) = (\pi/2, 0)$ and the other passes $(\theta_z, \theta_w) = (\pi/2, \pi/2)$. Most notably, when both p and q are nonzero, the line(s) winds around the torus in both the toroidal and poloidal directions, forming a knot when (p, q) are relatively prime, or links otherwise.

With these geometrical preparations, we are now ready to construct continuum models of nodal-knot semimetals. For continuum models, the momentum variables $\mathbf{k} = (k_x, k_y, k_z)$ extend to infinity. In the above construction of knot, the standard 3-sphere $n_1^2 + n_2^2 + n_3^2 + n_4^2 = 1$ is considered. To make use of this construction, we can compactify the $\mathbf{k}$-space to
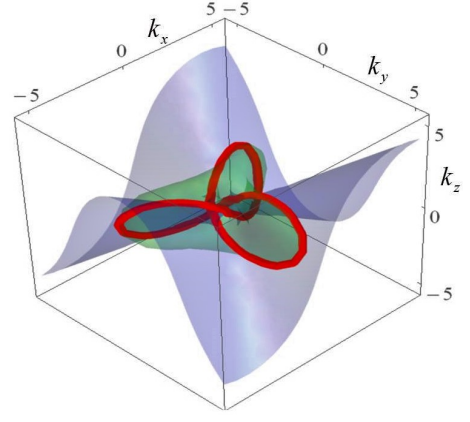

FIG. 2. The trefoil nodal knot of the continuum model in Eq.(9). The parameter m in Eq.(9) is $m = 0.5$. The green and blue surface is $a_1(\mathbf{k}) = 0$ and $a_3(\mathbf{k}) = 0$, respectively. Their intersection is the nodal knot.

3-sphere by adding an "infinity point" (This is a standard procedure in topology, which is essentially the converse of stereographic projection). We may establish a one-to-one correspondence between the compactified $\mathbf{k}$-space and the standard 3-sphere. There are infinitely many ways to do this; for instance, we can take

$$N_1 = k_x, \ N_2 = k_y, \ N_3 = k_z, \ N_4 = m - k^2/2, \tag{4}$$

with $k^2 = k_x^2 + k_y^2 + k_z^2$ and $m > 0$, and define $n_i = N_i/N$ with $N = \sqrt{N_1^2 + N_2^2 + N_3^2 + N_4^2}$. Now $\mathbf{n}(\mathbf{k}) = (n_1, n_2, n_3, n_4)$ maps the compactified $\mathbf{k}$-space to the standard 3-sphere. It maps the origin $\mathbf{k} = (0, 0, 0)$ to the north pole $\mathbf{n} = (0, 0, 0, 1)$, and the $\mathbf{k}$-infinity to the south pole $\mathbf{n} = (0, 0, 0, -1)$. The winding number of the mapping is known as

$$W = \frac{1}{2\pi^2}\int d^3k \, \epsilon^{abcd} n_a \partial_{k_x} n_b \partial_{k_y} n_c \partial_{k_z} n_d, \tag{5}$$

which is found to be -1 here. This is intuitively clear since the 3-sphere is covered only once. In fact, any other mapping with a nonzero winding number is applicable for our construction.

Now that $z = n_1 + in_2$ and $w = n_3 + in_4$ have become function of $\mathbf{k}$, we can take the coefficients a_1 and a_3 in Eq.(2) as functions of z and w. A natural choice is the real part and imaginary part of $f(z, w)$, respectively:

$$a_1(\mathbf{k}) = \mathrm{Re}f(z, w), \quad a_3(\mathbf{k}) = \mathrm{Im}f(z, w). \tag{6}$$

Eq.(3) and Eq.(6) are among the key equations of this paper. With this ansatz, the nodal line equation $a_1(\mathbf{k}) = a_3(\mathbf{k}) = 0$ is simply $f(z, w) = 0$, i.e., Eq.(3), which gives rise to a knot when (p, q) are relatively prime, as explained above. This is the motivation of the ansatz. To be simpler, we can take

$$z = N_1 + iN_2, \quad w = N_3 + iN_4 \tag{7}$$

in Eq.(6), which is topologically equivalent to taking $z = n_1 + in_2, w = n_3 + in_4$, because $\mathbf{n}(\mathbf{k})$ and $\mathbf{N}(\mathbf{k})$ differ only by a numerical factor $N(\mathbf{k})$. Hereafter we take the convention Eq.(7).
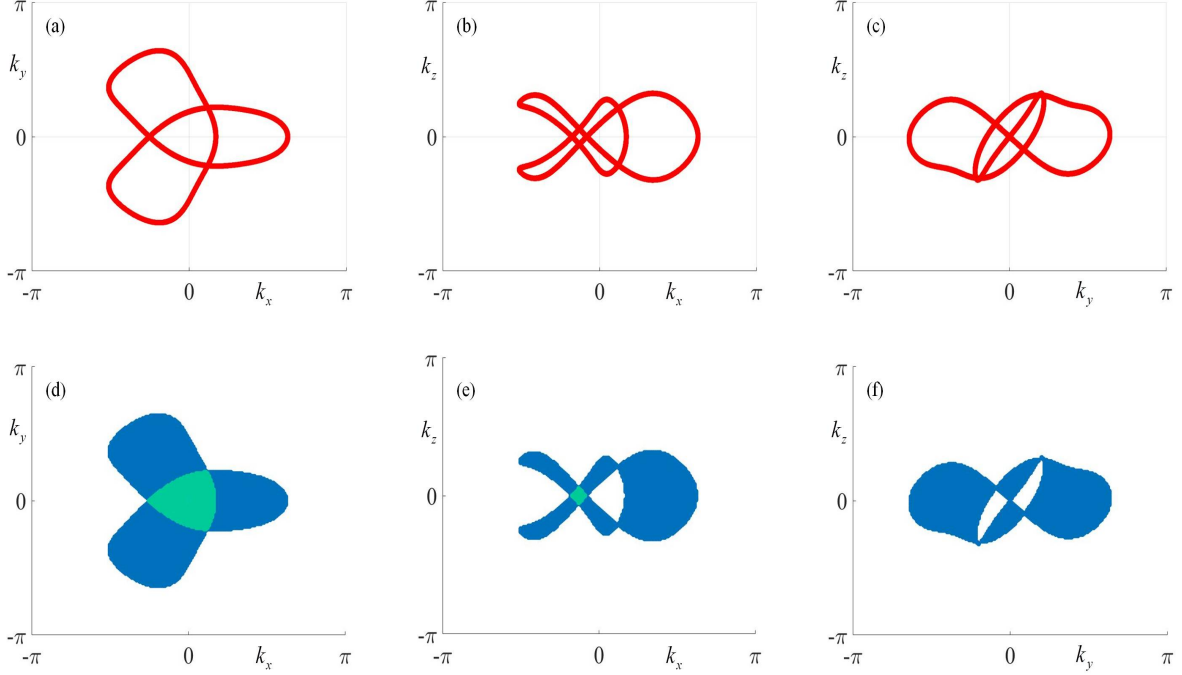
FIG. 3. (a)(b)(c) The projection of nodal knots to the surface Brillouin zone and (d)(e)(f) the regions of surface states, for the three spatial directions. In the blue regions in (d),(e), and (f), there is one surface band; in the green regions, there are two. The Bloch Hamiltonian is Eq.(2) with a_1, a_3 given by Eq.(11); $m_0 = 2.5$.

In the case $(p, q) = (3, 2)$, we have $f(z, w) = (N_1 + iN_2)^3 + (N_3 + iN_4)^2$, and the ansatz in Eq.(6) leads to

$$a_1(\mathbf{k}) = N_1^3 - 3N_1N_2^2 + N_3^2 - N_4^2,$$
$$a_3(\mathbf{k}) = 3N_1^2N_2 - N_2^3 + 2N_3N_4, \tag{8}$$

thus the Bloch Hamiltonian reads

$$H(\mathbf{k}) = [k_x^3 - 3k_xk_y^2 + k_z^2 - (m - k^2/2)^2]\sigma_x$$
$$+ [3k_x^2k_y - k_y^3 + 2k_z(m - k^2/2)]\sigma_z, \tag{9}$$

where $k^2 = \sum_{i=x,y,z} k_i^2$. The nodal line of this model is shown in Fig.2, which is apparently a trefoil nodal knot. Many other nodal knots can be obtained in this way by taking other (p, q) or $\mathbf{N}(\mathbf{k})$ function.

III. LATTICE MODELS OF NODAL-KNOT SEMIMETALS AND KNOTTED-UNKNOTTED TOPOLOGICAL TRANSITIONS

For lattice models, the $\mathbf{k}$-space (Brillouin zone) is a 3-torus T^3. The main difference compared to the continuum model is that $\mathbf{N}(\mathbf{k})$ must be periodic in $\mathbf{k}$, otherwise the construction is similar. Following the lead of Eq.(4), we can take

$$N_1 = \sin k_x, \ N_2 = \sin k_y, \ N_3 = \sin k_z,$$
$$N_4 = \cos k_x + \cos k_y + \cos k_z - m_0. \tag{10}$$

Expanding N_4 in Eq.(10) to the first order, we can see that $3 - m_0$ plays the role of m. The same Eq.(6) gives rise to

models of nodal knots in lattice models. According to Eq.(6), the Bloch Hamiltonian for the simplest case $(p, q) = (3, 2)$ is given by Eq.(2) with

$$a_1(\mathbf{k}) = \sin^2 k_z - (\sum_i \cos k_i - m_0)^2 + \sin^3 k_x - 3\sin k_x \sin^2 k_y,$$
$$a_3(\mathbf{k}) = 2\sin k_z(\sum_i \cos k_i - m_0) + 3\sin^2 k_x \sin k_y - \sin^3 k_y. \tag{11}$$

It hosts a nodal knot for $1 < m_0 < 3$ (in this regime, the previously defined winding number $W = -1$). The nodal knot of $m_0 = 2.5$ is already shown in Fig.1(d) as a representative of nodal knots. The presence of nodal knots implies the existence of interesting surface states. These flat-band surface states are shown in Fig.3. It is apparent that the $\mathbf{k}$-space boundary of the surface-state bands is the projection of nodal knot to the surface Brillouin zone.

It is also interesting to investigate the topological transition from the unknotted nodal lines to the knotted ones. To this end, we add an additional σ_z term into the Bloch Hamiltonian:

$$a_1(\mathbf{k}) = \sin^2 k_z - (\sum_i \cos k_i - m_0)^2 + \sin^3 k_x - 3\sin k_x \sin^2 k_y,$$
$$a_3(\mathbf{k}) = 2\sin k_z(\sum_i \cos k_i - m_0) + 3\sin^2 k_x \sin k_y$$
$$- \sin^3 k_y + m_z\sigma_z. \tag{12}$$

The evolution of nodal knot as a function of m_z is shown in Fig.4. As we increase m_z, the nodal knot gradually deforms.
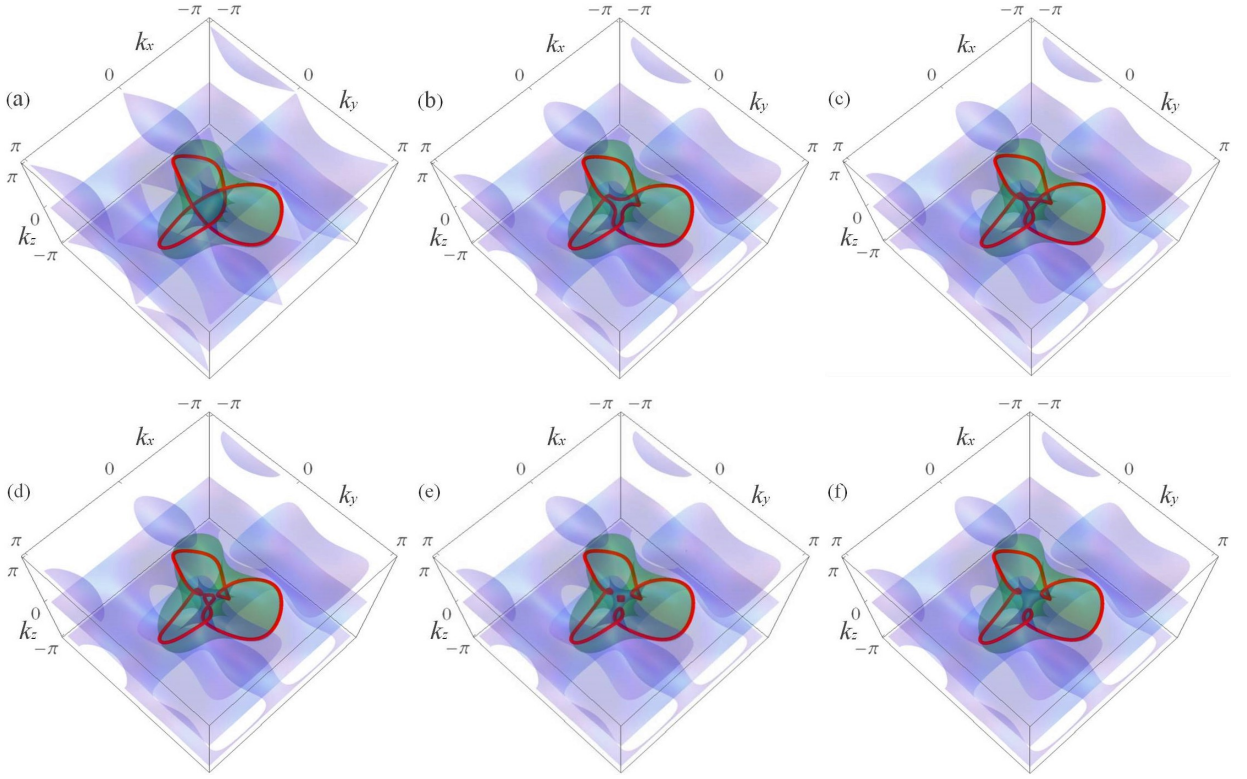
FIG. 4. The evolution of nodal knot as a function of m_z. Here, $m_0 = 2.7$ is fixed. (a) $m_z = 0$, (b) $m_z = 0.1200$, (c) $m_z = 0.1316$, (d) $m_z = 0.1323$, (e) $m_z = 0.1370$, (f) $m_z = 0.1400$. The green and blue surface is defined by $a_1(\mathbf{k}) = 0$ and $a_3(\mathbf{k}) = 0$, respectively. The knotted-unknotted transition occurs through nodal-line reconnections, which is clear in (b)(c)(d).

Around $m_z \approx 0.13$, there are three successive nodal-line reconnection transitions, taking places at three different locations in the Brillouin zone. After the nodal-line reconnections, the original nodal knot evolves to two nodal rings. As we further increase m_z, the smaller ring shrinks and finally disappears [Fig.4(d)(e)]. At $m_z = 0.14$, we have a single unknotted nodal line [Fig.4(f)].

We have focused on the simplest case $(p, q) = (3, 2)$ for simplicity. In fact, the method is general and applicable to all other pairs of integers. As we have explained, nodal knots can be obtained when (p, q) are relatively prime, otherwise nodal links are obtained. We have shown the nodal lines for several choices of (p, q) in Fig.5. In Fig.5(a)(b)(c), different shapes of nodal knots can be found. In contrast, Fig.5(d) is a nodal link due to the fact that 4 and 2 are not relatively prime.

IV. FINAL REMARKS

Knots are often studied in the real space. In this paper, we have introduced knots in the momentum space (Brillouin zone), in the context of topological semimetals. Here, the nodal knots emerge as the knotted band-crossing lines. These topological semimetals have been dubbed "nodal-knot semimetals" in this paper, to distinguish them for the ordinary nodal-line semimetals with unknotted nodal lines. We hope that this work can stimulate further applications of the rich
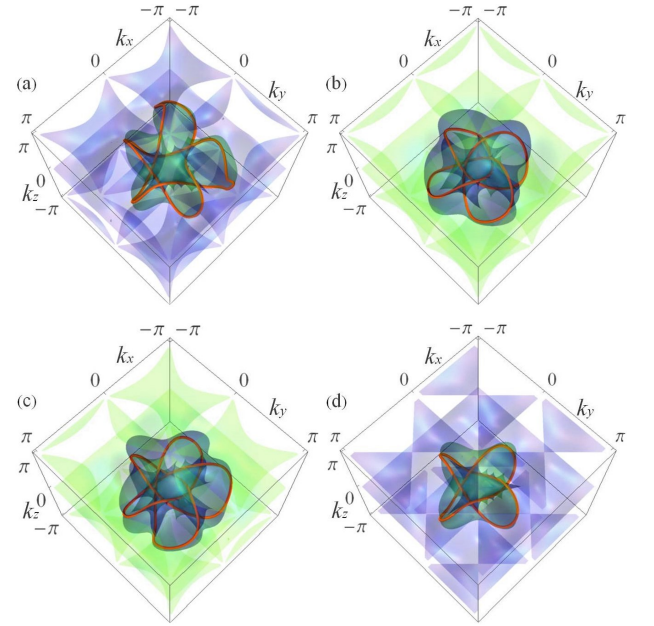

FIG. 5. Nodal knots for several values of (p, q). The Hamiltonian is given by the ansatz Eq.(6); $m_0 = 2.5$. (a) $(p, q) = (5, 3)$; (b) $(p, q) = (4, 3)$; (c) $(p, q) = (5, 2)$; (d) $(p, q) = (4, 2)$. In (a),(b),(c) we have a nodal knot (a single knotted nodal line), while in (d) we have a nodal link. In the cases (a),(b), and (c), p and q are relatively prime.

subject of knot theory[70] to topological semimetals.

In this work, we have taken a function of two complex variables to construct nodal knots in three-dimensional Brillouin zone; theoretically, it may be interesting to generalize this method to higher dimensions (with possibly more complex variables).

Noted added.–Upon completing this manuscript, we become aware of a preprint studying nodal knots using a different approach[85]. Unlike the everywhere smooth Bloch Hamiltonian here, their trefoil-nodal-knot Hamiltonian has a discontinuity in the Brillouin zone (a square-root branch cut).

[1] M. Z. Hasan and C. L. Kane, "*Colloquium* : Topological insulators," Rev. Mod. Phys. **82**, 3045–3067 (2010).

[2] Xiao-Liang Qi and Shou-Cheng Zhang, "Topological insulators and superconductors," Rev. Mod. Phys. **83**, 1057–1110 (2011).

[3] A. Bansil, Hsin Lin, and Tanmoy Das, "*Colloquium* : Topological band theory," Rev. Mod. Phys. **88**, 021004 (2016).

[4] B Andrei Bernevig and Taylor L Hughes, *Topological insulators and topological superconductors* (Princeton University Press, 2013).

[5] Shun-Qing Shen, *Topological Insulators: Dirac Equation in Condensed Matters*, Vol. 174 (Springer Science & Business Media, 2013).

[6] Ching-Kai Chiu, Jeffrey C. Y. Teo, Andreas P. Schnyder, and Shinsei Ryu, "Classification of topological quantum matter with symmetries," Rev. Mod. Phys. **88**, 035005 (2016).

[7] Shuichi Murakami and Shun-ichi Kuga, "Universal phase diagrams for the quantum spin hall systems," Phys. Rev. B **78**, 165313 (2008).

[8] Xiangang Wan, Ari M. Turner, Ashvin Vishwanath, and Sergey Y. Savrasov, "Topological semimetal and fermi-arc surface states in the electronic structure of pyrochlore iridates," Phys. Rev. B **83**, 205101 (2011).

[9] A. A. Burkov and Leon Balents, "Weyl semimetal in a topological insulator multilayer," Phys. Rev. Lett. **107**, 127205 (2011).

[10] Kai-Yu Yang, Yuan-Ming Lu, and Ying Ran, "Quantum hall effects in a weyl semimetal: Possible application in pyrochlore iridates," Phys. Rev. B **84**, 075129 (2011).

[11] G. E. Volovik, *The Universe in a Helium Droplet* (Oxford University Press,USA, 2003).

[12] Hongming Weng, Chen Fang, Zhong Fang, B. Andrei Bernevig, and Xi Dai, "Weyl semimetal phase in noncentrosymmetric transition-metal monophosphides," Phys. Rev. X **5**, 011029 (2015).

[13] S.-M. Huang, S.-Y. Xu, I. Belopolski, C.-C. Lee, G. Chang, B. Wang, N. Alidoust, G. Bian, M. Neupane, A. Bansil, H. Lin, and M. Zahid Hasan, "An inversion breaking Weyl semimetal state in the TaAs material class," Nature Communications **6**, 7373 (2015).

[14] Su-Yang Xu, Ilya Belopolski, Nasser Alidoust, Madhab Neupane, Guang Bian, Chenglong Zhang, Raman Sankar, Guoqing Chang, Zhujun Yuan, Chi-Cheng Lee, *et al.*, "Discovery of a weyl fermion semimetal and topological fermi arcs," Science **349**, 613–617 (2015).

[15] BQ Lv, HM Weng, BB Fu, XP Wang, H Miao, J Ma, P Richard, XC Huang, LX Zhao, GF Chen, *et al.*, "Experimental discovery of weyl semimetal taas," Physical Review X **5**, 031013 (2015).

[16] Xiaochun Huang, Lingxiao Zhao, Yujia Long, Peipei Wang, Dong Chen, Zhanhai Yang, Hui Liang, Mianqi Xue, Hongming Weng, Zhong Fang, Xi Dai, and Genfu Chen, "Observation of the chiral-anomaly-induced negative magnetoresistance in 3d weyl semimetal taas," Phys. Rev. X **5**, 031023 (2015).

[17] S.-Y. Xu, N. Alidoust, I. Belopolski, C. Zhang, G. Bian, T.-R. Chang, H. Zheng, V. Strokov, D. S. Sanchez, G. Chang, Z. Yuan, D. Mou, Y. Wu, L. Huang, C.-C. Lee, S.-M. Huang, B. Wang, A. Bansil, H.-T. Jeng, T. Neupert, A. Kaminski, H. Lin, S. Jia, and M. Zahid Hasan, "Discovery of Weyl semimetal NbAs," ArXiv e-prints (2015), arXiv:1504.01350 [cond-mat.mes-hall].

[18] LX Yang, ZK Liu, Yan Sun, Han Peng, HF Yang, Teng Zhang, Bo Zhou, Yi Zhang, YF Guo, Marein Rahn, *et al.*, "Weyl semimetal phase in the non-centrosymmetric compound taas," Nature physics **11**, 728–732 (2015).

[19] Chandra Shekhar, Ajaya K Nayak, Yan Sun, Marcus Schmidt, Michael Nicklas, Inge Leermakers, Uli Zeitler, Yurii Skourski, Jochen Wosnitza, Zhongkai Liu, *et al.*, "Extremely large magnetoresistance and ultrahigh mobility in the topological weyl semimetal candidate nbp," Nature Physics **11**, 645–649 (2015).

[20] Ling Lu, Zhiyu Wang, Dexin Ye, Lixin Ran, Liang Fu, John D. Joannopoulos, and Marin Soljačić, "Experimental observation of weyl points," **349**, 622–624 (2015).

[21] Alexey A Soluyanov, Dominik Gresch, Zhijun Wang, Quan-Sheng Wu, Matthias Troyer, Xi Dai, and B Andrei Bernevig, "Type-ii weyl semimetals," Nature **527**, 495–498 (2015).

[22] M. Neupane, S.-Y. Xu, R. Sankar, N. Alidoust, G. Bian, C. Liu, I. Belopolski, T.-R. Chang, H.-T. Jeng, H. Lin, A. Bansil, F. Chou, and M. Z. Hasan, "Observation of a three-dimensional topological Dirac semimetal phase in high-mobility Cd_3As_2," Nature Communications **5**, 3786 (2014), arXiv:1309.7892 [cond-mat.mes-hall].

[23] Su-Yang Xu, Chang Liu, Satya K Kushwaha, Raman Sankar, Jason W Krizan, Ilya Belopolski, Madhab Neupane, Guang Bian, Nasser Alidoust, Tay-Rong Chang, *et al.*, "Observation of fermi arc surface states in a topological metal," Science **347**, 294–298 (2015).

[24] ZK Liu, B Zhou, Y Zhang, ZJ Wang, HM Weng, D Prabhakaran, S-K Mo, ZX Shen, Z Fang, X Dai, *et al.*, "Discovery of a three-dimensional topological dirac semimetal, na3bi," Science **343**, 864–867 (2014).

[25] Sergey Borisenko, Quinn Gibson, Danil Evtushinsky, Volodymyr Zabolotnyy, Bernd Büchner, and Robert J. Cava, "Experimental realization of a three-dimensional dirac semimetal," Phys. Rev. Lett. **113**, 027603 (2014).

[26] Steve M Young, Saad Zaheer, Jeffrey CY Teo, Charles L Kane, Eugene J Mele, and Andrew M Rappe, "Dirac semimetal in three dimensions," Physical review letters **108**, 140405 (2012).

[27] Zhijun Wang, Yan Sun, Xing-Qiu Chen, Cesare Franchini, Gang Xu, Hongming Weng, Xi Dai, and Zhong Fang, "Dirac semimetal and topological phase transitions in a 3 bi (a= na, k, rb)," Physical Review B **85**, 195320 (2012).

[28] Zhijun Wang, Hongming Weng, Quansheng Wu, Xi Dai, and

Zhong Fang, "Three-dimensional dirac semimetal and quantum transport in cd 3 as 2," Physical Review B **88**, 125427 (2013).

[29] R. Y. Chen, Z. G. Chen, X.-Y. Song, J. A. Schneeloch, G. D. Gu, F. Wang, and N. L. Wang, "Magnetoinfrared spectroscopy of landau levels and zeeman splitting of three-dimensional massless dirac fermions in zrte$_5$," Phys. Rev. Lett. **115**, 176404 (2015).

[30] Yanwen Liu, Xiang Yuan, Cheng Zhang, Zhao Jin, Awadhesh Narayan, Chen Luo, Zhigang Chen, Lei Yang, Jin Zou, Xing Wu, *et al.*, "Zeeman splitting and dynamical mass generation in dirac semimetal zrte5," Nature communications **7**, 12516 (2016).

[31] A. A. Burkov, M. D. Hook, and Leon Balents, "Topological nodal semimetals," Phys. Rev. B **84**, 235126 (2011).

[32] Michael Phillips and Vivek Aji, "Tunable line node semimetals," Phys. Rev. B **90**, 115111 (2014).

[33] Jean-Michel Carter, V. Vijay Shankar, M. Ahsan Zeb, and Hae-Young Kee, "Semimetal and topological insulator in perovskite iridates," Phys. Rev. B **85**, 115105 (2012).

[34] Ching-Kai Chiu and Andreas P. Schnyder, "Classification of reflection-symmetry-protected topological semimetals and nodal superconductors," Phys. Rev. B **90**, 205136 (2014).

[35] M. Zeng, C. Fang, G. Chang, Y.-A. Chen, T. Hsieh, A. Bansil, H. Lin, and L. Fu, "Topological semimetals and topological insulators in rare earth monopnictides," ArXiv e-prints (2015), arXiv:1504.03492 [cond-mat.mes-hall].

[36] Yige Chen, Yuan-Ming Lu, and Hae-Young Kee, "Topological crystalline metal in orthorhombic perovskite iridates," Nature communications **6**, 6593 (2015).

[37] Hongming Weng, Yunye Liang, Qiunan Xu, Rui Yu, Zhong Fang, Xi Dai, and Yoshiyuki Kawazoe, "Topological node-line semimetal in three-dimensional graphene networks," Phys. Rev. B **92**, 045108 (2015).

[38] G. Bian, T.-R. Chang, R. Sankar, S.-Y. Xu, H. Zheng, T. Neupert, C.-K. Chiu, S.-M. Huang, G. Chang, I. Belopolski, D. S. Sanchez, M. Neupane, N. Alidoust, C. Liu, B. Wang, C.-C. Lee, H.-T. Jeng, A. Bansil, F. Chou, H. Lin, and M. Zahid Hasan, "Topological nodal-line fermions in spin-orbit metal PbTaSe2," Nature Communications **7**, 10556 (2016).

[39] Rui Yu, Hongming Weng, Zhong Fang, Xi Dai, and Xiao Hu, "Topological node-line semimetal and dirac semimetal state in antiperovskite cu$_3$PdN," Phys. Rev. Lett. **115**, 036807 (2015).

[40] Youngkuk Kim, Benjamin J. Wieder, C. L. Kane, and Andrew M. Rappe, "Dirac line nodes in inversion-symmetric crystals," Phys. Rev. Lett. **115**, 036806 (2015).

[41] Jun-Won Rhim and Yong Baek Kim, "Landau level quantization and almost flat modes in three-dimensional semimetals with nodal ring spectra," Phys. Rev. B **92**, 045126 (2015).

[42] Y. Chen, Y. Xie, S. A. Yang, H. Pan, F. Zhang, M. L. Cohen, and S. Zhang, "Spin-orbit-free Weyl-loop and Weyl-point semimetals in a stable three-dimensional carbon allotrope," ArXiv e-prints (2015), arXiv:1505.02284 [cond-mat.mtrl-sci].

[43] Chen Fang, Yige Chen, Hae-Young Kee, and Liang Fu, "Topological nodal line semimetals with and without spin-orbital coupling," Phys. Rev. B **92**, 081201 (2015).

[44] Kieran Mullen, Bruno Uchoa, and Daniel T. Glatzhofer, "Line of dirac nodes in hyperhoneycomb lattices," Phys. Rev. Lett. **115**, 026403 (2015).

[45] Guang Bian, Tay-Rong Chang, Hao Zheng, Saavanth Velury, Su-Yang Xu, Titus Neupert, Ching-Kai Chiu, Shin-Ming Huang, Daniel S. Sanchez, Ilya Belopolski, Nasser Alidoust, Peng-Jen Chen, Guoqing Chang, Arun Bansil, Horng-Tay Jeng, Hsin Lin, and M. Zahid Hasan, "Drumhead surface states and topological nodal-line fermions in tltase$_2$,"

[46] Rui Yu, Zhong Fang, Xi Dai, and Hongming Weng, "Topological nodal line semimetals predicted from first-principles calculations," Frontiers of Physics **12**, 127202 (2017).

[47] Lilia S. Xie, Leslie M. Schoop, Elizabeth M. Seibel, Quinn D. Gibson, Weiwei Xie, and Robert J. Cava, "A new form of ca3p2 with a ring of dirac nodes," APL Mater. **3**, 083602 (2015).

[48] Y.-H. Chan, Ching-Kai Chiu, M. Y. Chou, and Andreas P. Schnyder, "ca$_3$p$_2$ and other topological semimetals with line nodes and drumhead surface states," Phys. Rev. B **93**, 205132 (2016).

[49] J. L. Lu, W. Luo, X. Y. Li, S. Q. Yang, J. X. Cao, X. G. Gong, and H. J. Xiang, "Two-Dimensional Node-Line Semimetals in a Honeycomb-Kagome Lattice," ArXiv e-prints (2016), arXiv:1603.04596 [cond-mat.mtrl-sci].

[50] Qiunan Xu, Rui Yu, Zhong Fang, Xi Dai, and Hongming Weng, "Topological nodal line semimetals in the cap$_3$ family of materials," Phys. Rev. B **95**, 045136 (2017).

[51] Ronghan Li, Hui Ma, Xiyue Cheng, Shoulong Wang, Dianzhong Li, Zhengyu Zhang, Yiyi Li, and Xing-Qiu Chen, "Dirac node lines in pure alkali earth metals," Phys. Rev. Lett. **117**, 096401 (2016).

[52] Motoaki Hirayama, Ryo Okugawa, Takashi Miyake, and Shuichi Murakami, "Topological dirac nodal lines and surface charges in fcc alkaline earth metals," Nature Communications **8**, 14022 (2017).

[53] Jin Hu, Zhijie Tang, Jinyu Liu, Xue Liu, Yanglin Zhu, David Graf, Yanmeng Shi, Shi Che, Chun Ning Lau, Jiang Wei, *et al.*, "Topological nodal-line fermions in zrsise and zrsite," arXiv preprint arXiv:1604.06860 (2016).

[54] Leslie M Schoop, Mazhar N Ali, Carola Straßer, Viola Duppel, Stuart SP Parkin, Bettina V Lotsch, and Christian R Ast, "Dirac cone protected by non-symmorphic symmetry and 3d dirac line node in zrsis," arXiv preprint arXiv:1509.00861 (2015).

[55] R. Singha, A. Pariari, B. Satpati, and P. Mandal, "Titanic magnetoresistance and signature of non-degenerate Dirac nodes in ZrSiS," ArXiv e-prints (2016), arXiv:1602.01993 [cond-mat.mtrl-sci].

[56] Madhab Neupane, Ilya Belopolski, M. Mofazzel Hosen, Daniel S. Sanchez, Raman Sankar, Maria Szlawska, Su-Yang Xu, Klauss Dimitri, Nagendra Dhakal, Pablo Maldonado, Peter M. Oppeneer, Dariusz Kaczorowski, Fangcheng Chou, M. Zahid Hasan, and Tomasz Durakiewicz, "Observation of topological nodal fermion semimetal phase in zrsis," Phys. Rev. B **93**, 201104 (2016).

[57] X. Wang, X. Pan, M. Gao, J. Yu, J. Jiang, J. Zhang, H. Zuo, M. Zhang, Z. Wei, W. Niu, Z. Xia, X. Wan, Y. Chen, F. Song, Y. Xu, B. Wang, G. Wang, and R. Zhang, "Evidence of both surface and bulk Dirac bands in ZrSiS and the unconventional magnetoresistance," ArXiv e-prints (2016), arXiv:1604.00108 [cond-mat.mtrl-sci].

[58] C Chen, X Xu, J Jiang, S-C Wu, YP Qi, LX Yang, MX Wang, Y Sun, NBM Schröter, HF Yang, *et al.*, "Dirac line nodes and effect of spin-orbit coupling in the nonsymmorphic critical semimetals msis (m=hf, zr)," Physical Review B **95**, 125126 (2017).

[59] Zhongbo Yan and Zhong Wang, "Tunable weyl points in periodically driven nodal line semimetals," Phys. Rev. Lett. **117**, 087402 (2016).

[60] Ching-Kit Chan, Yun-Tak Oh, Jung Hoon Han, and Patrick A. Lee, "Type-ii weyl cone transitions in driven semimetals," Phys. Rev. B **94**, 121106 (2016).

[61] Awadhesh Narayan, "Tunable point nodes from line-node semimetals via application of light,"

Phys. Rev. B **94**, 041409 (2016).

[62] X.-X. Zhang, T. Tzen Ong, and N. Nagaosa, "Theory of photoinduced Floquet Weyl semimetal phases," ArXiv e-prints (2016), arXiv:1607.05941 [cond-mat.mtrl-sci].

[63] Katsuhisa Taguchi, Dong-Hui Xu, Ai Yamakage, and K. T. Law, "Photovoltaic anomalous hall effect in line-node semimetals," Phys. Rev. B **94**, 155206 (2016).

[64] T. Bzdušek, Q. Wu, A. Rüegg, M. Sigrist, and A. A. Soluyanov, "Nodal-chain metals," Nature (London) **538**, 75–78 (2016), arXiv:1604.03112 [cond-mat.mes-hall].

[65] R. Yu, Q. Wu, Z. Fang, and H. Weng, "From Nodal Chain Semimetal To Weyl Semimetal in HfC," ArXiv e-prints (2017), arXiv:1701.08502 [cond-mat.mtrl-sci].

[66] Wei Chen, Hai-Zhou Lu, and Jing-Min Hou, "Topological hopf-link semimetal," arXiv preprint arXiv:1703.10886 (2017).

[67] Z. Yan, R. Bi, H. Shen, L. Lu, S.-C. Zhang, and Z. Wang, "Nodal-link semimetals," ArXiv e-prints (2017), arXiv:1704.00655 [cond-mat.str-el].

[68] P.-Y. Chang and C.-H. Yee, "Weyl-link semimetals," ArXiv e-prints (2017), arXiv:1704.01948 [cond-mat.mes-hall].

[69] X.-Q. Sun, B. Lian, and S.-C. Zhang, "Double helix nodal line superconductor," ArXiv e-prints (2017), arXiv:1704.01661 [cond-mat.supr-con].

[70] Louis H Kauffman, *Knots and physics*, Vol. 1 (World scientific, 2001).

[71] Petr Hořava, "Stability of fermi surfaces and k theory," Phys. Rev. Lett. **95**, 016405 (2005).

[72] Y. X. Zhao and Z. D. Wang, "Topological classification and stability of fermi surfaces," Phys. Rev. Lett. **110**, 240404 (2013).

[73] Y. X. Zhao, Andreas P. Schnyder, and Z. D. Wang, "Unified theory of pt and cp invariant topological metals and nodal superconductors," Phys. Rev. Lett. **116**, 156402 (2016).

[74] Y. X. Zhao and Y. Lu, "Pt-symmetric real dirac fermions and semimetals," Phys. Rev. Lett. **118**, 056401 (2017).

[75] K. Li, C. Li, J. Hu, Y. Li, and C. Fang, "Dirac and nodal-line magnons in collinear antiferromagnets," ArXiv e-prints (2017), arXiv:1703.08545 [cond-mat.mes-hall].

[76] Frank Wilczek and A. Zee, "Linking numbers, spin, and statistics of solitons," Phys. Rev. Lett. **51**, 2250–2252 (1983).

[77] Mikio Nakahara, *Geometry, topology and physics* (CRC Press, 2003).

[78] Joel E Moore, Ying Ran, and Xiao-Gang Wen, "Topological surface states in three-dimensional magnetic insulators," Physical review letters **101**, 186805 (2008).

[79] D.-L. Deng, S.-T. Wang, C. Shen, and L.-M. Duan, "Hopf insulators and their topologically protected surface states," Phys. Rev. B **88**, 201105 (2013).

[80] D.-L. Deng, S.-T. Wang, K. Sun, and L.-M. Duan, "Probe knots and Hopf insulators with ultracold atoms," ArXiv e-prints (2016), arXiv:1612.01518 [cond-mat.mes-hall].

[81] D.-L. Deng, S.-T. Wang, and L.-M. Duan, "Systematic construction of tight-binding hamiltonians for topological insulators and superconductors," Phys. Rev. B **89**, 075126 (2014).

[82] Ricardo Kennedy, "Topological hopf-chern insulators and the hopf superconductor," Phys. Rev. B **94**, 035137 (2016).

[83] C. Wang, P. Zhang, X. Chen, J. Yu, and H. Zhai, "Measuring Topological Number of a Chern-Insulator from Quench Dynamics," ArXiv e-prints (2016), arXiv:1611.03304 [cond-mat.quant-gas].

[84] C. Liu, F. Vafa, and C. Xu, "Symmetry Protected Topological Hopf Insulator and its Generalizations," ArXiv e-prints (2016), arXiv:1612.04905 [cond-mat.str-el].

[85] M. Ezawa, "Topological Semimetals carrying Arbitrary Hopf Numbers: Hopf-Link, Solomon's-Knot, Trefoil-Knot and Other Semimetals," ArXiv e-prints (2017), arXiv:1704.04941 [cond-mat.mes-hall].